Cardiovascular Revascularization Medicine 20 (2019) 768–774

Contents lists available at ScienceDirect

Cardiovascular Revascularization Medicine

The Impact of Blood Pressure Variability on Coronary Arterial Lumen Dimensions as Assessed by Optical Coherence Tomography in Patients with ST-Elevation Myocardial Infarction

Mohamad Soud [a], Giovanni L. De Maria [b,c], Hector M. Garcia-Garcia [a,*], Stefano Benenati [b], Keith M. Channon [b], Kayode Kuku [a], Yuichi Ozaki [a], Muhammad Ali Tariq [a], Jouke Dijkstra [d], Alexandre Hideo-Kajita [a], Oxford Acute Myocardial Infarction (OxAMI) Study investigators , Adrian P. Banning [b,**]

[a] MedStar Heart & Vascular Institute, MedStar Washington Hospital Center, Washington, DC, USA
[b] Oxford Heart Centre, NIHR Biomedical Research Centre, Oxford University Hospitals, Oxford, UK
[c] Cardiovascular Department, Università Cattolica del Sacro Cuore, Rome, Italy
[d] LKEB, Leiden University, Leiden, the Netherlands

ARTICLE INFO

Article history:
Received 8 March 2019
Received in revised form 15 May 2019
Accepted 28 May 2019

ABSTRACT

Background: Patients with ST-elevation Myocardial Infarction treated by primary percutaneous coronary intervention (PPCI) experience drastic hemodynamic systemic changes (i.e., blood pressure) during the different phases of the procedure. Optical coherence tomography is often used to unveil the underlying cause of STEMI (pre-PCI) and to optimize stent implantation (post-PCI). The impact of blood pressure variability on coronary lumen remains uncertain. This study aimed to investigate the relationship between blood pressure variability, before and after PCI, and coronary arterial lumen dimensions of the infarct-related artery.
Methods: We measured systolic, diastolic and mean arterial blood pressure (SBP, DBP, and MAP; respectively) at pre- and post-PCI. Frequency-domain optical coherence tomography (FD-OCT) imaging was performed at the same time points. Offline quantitative image analyses were performed to assess the average and minimum lumen area (LA). Δ blood pressure (after and before the PCI) was then calculated.
Results: A total of 14 ST-segment elevation myocardial infarction (STEMI) patients were included. 84.2% of enrolled patients were male with a mean age of (58 ± 10.7 years). Roughly two-thirds (57.8%) had hypertension. The mean SBP was (112.6 mm Hg ± 16.1) and (117.2 mm Hg ± 20.9), pre- and post-stenting, respectively; the range of the observed SBP differences (between pre- and post-PCI) went from −25 to +23 mm Hg. Pre- and post-stenting mean average LA were (7.1 ± 2.5 mm^2 and 6.8 ± 2.3 mm^2; respectively). There were poor correlations between ΔSBP and Δ mean minimum LA. A similar pattern was observed with ΔDBP and ΔMAP.
Conclusion: Despite significant hemodynamic variability, the difference in lumen cross-sectional area, between pre- and post-coronary artery stenting was minimal. This study supports the use of OCT lumen areas to inform clinical decisions during PPCI.

1. Introduction

The introduction of OCT into the catheterization laboratory has been received with great expectation, as this light-based imaging modality offers ten times higher resolution and 40 times faster imaging acquisition compared with intravascular ultrasound [1,2]. However, the first-generation time-domain OCT (TD-OCT) was plagued with the requirement of proximal balloon occlusion to limit antegrade blood. Today, the frequency-domain OCT (FD-OCT) has overcome the inherent technical limitations of TD-OCT with the development of high acquisition speed that alleviated the need for proximal balloon occlusion, thus simplifying the use of the technology by using contrast media injection. These new acquisition techniques have allowed for widespread clinical applications, including assessment of plaque morphology and guidance of stent placement during percutaneous coronary interventions (PCI) in ST-elevation Myocardial Infarction (STEMI) patients [3–6]. Some of the guidance parameters, such as stent sizing and stent optimization, rely on the assessment of luminal dimensions.

* Correspondence to: H. M. Garcia-Garcia, Interventional Cardiology, MedStar Washington Hospital Center, 110 Irving St NW, Washington, DC 20010, USA.
** Correspondence to: A. P. Banning, Oxford Heart Centre, Oxford University Hospitals, Headley Way, Oxford OX39DU, UK.
E-mail addresses: Hector.M.GarciaGarcia@medstar.net (H.M. Garcia-Garcia), adrian.banning@ouh.nhs.uk (A.P. Banning).

https://doi.org/10.1016/j.carrev.2019.05.027
1553-8389/

ST-elevation Myocardial Infarction (STEMI) patients treated with primary percutaneous coronary interventions (PPCI) experience drastic hemodynamic systemic changes during the procedure. The impact of blood pressure variability on coronary lumen dimensions remains uncertain. We sought, therefore, to investigate the relationship between blood pressure variability, during primary PCI, and coronary arterial lumen dimensions of the infarct-related artery as assessed by non-occlusive FD-OCT imaging.

2. Methods

2.1. Patient population

We conducted a post hoc analysis of the original data of prospectively enrolled patients who were recruited as part of the Oxford Acute Myocardial Infarction (Ox-AMI) study (REC number 10/H0408/24). The methods and data relating to this cohort have been published previously. [7]

Briefly, the study population consisted of 82 prospectively enrolled patients with STEMI who underwent PPCI at the Oxford Radcliffe University Hospitals (Oxford, United Kingdom) from January 2014 to July 2014. STEMI was defined as the occurrence of ongoing chest pain for at least 30 min associated with ST-segment elevation >2 mm in at least two contiguous leads. All patients underwent PPCI with stent implantation. Decisions about direct stenting technique, thrombectomy and glycoprotein (GP) IIb/IIIa inhibitor adoption were left to operator discretion. All patients were loaded with aspirin 300 mg and clopidogrel 600 mg or ticagrelor 180 mg. Weight-adjusted unfractionated heparin or bivalirudin was administered.

Exclusion criteria were symptoms duration >12 h, presence of cardiogenic shock, severe left main disease, contraindications to adenosine infusion, plain old balloon angioplasty without stent implantation, known history of severe chronic kidney disease (estimated glomerular filtration rate < 30 ml/min), severe tortuous vessel or unfavorable anatomy for an FD-OCT study. The local ethics committee approved the protocol, and the study was carried out in accordance with the Declaration of Helsinki.

2.2. Percutaneous coronary intervention

PPCI was performed according to international guidelines. All patients were loaded with a double-antiplatelet treatment at the time of the procedure (600 mg of Clopidogrel and 300 mg of Aspirin in the ambulance). Anticoagulation was achieved with Bivalirudin (0.75 mg/kg bolus, followed by an infusion of 1.75 mg/kg/min for up four h after the procedure as clinically warranted). Both the use of Abciximab and thrombus aspiration were left to the operator's discretion.

2.3. Angiographic and ECG analysis

Pre-stenting residual stenosis was measured by two-dimensional quantitative coronary angiography (Medcon QCA software; Medcon Limited, Tel Aviv, Israel). Baseline preprocedural angiographic thrombus burden was graded from 0 to 5 by the thrombus score as described previously [8]. Pre-PPCI and final thrombolysis in myocardial infarction flow and post-procedural MBG were assessed. Angiographic distal embolization was defined as the occurrence of a distal filling defect with an abrupt 'cut-off' appearance in one or more peripheral branches of the infarct-related artery distal to the PPCI site [9].

A 12 lead ECG was recorded at admission, and 60 min after PPCI in all patients and ST resolution (ΣSTR) was calculated as described previously, ΣSTR being defined as incomplete if <70% [10].

2.4. Measurement hemodynamics parameters

Before proceeding with stenting, and after intracoronary injection of 250 μg of isosorbide dinitrate, the following baseline parameters were measured: systolic blood pressure (SBP), diastolic blood pressure (DBP), and mean arterial pressure (MAP). The same parameters were measured again after hyperemia, induced by an intravenous infusion of adenosine at a rate of 140 μg/kg/min.

Post-dilation was left to the operator's discretion. When the operator was satisfied with the procedural result, SBP, DBP, and MAP were measured again at baseline and after hyperemia induction.

Indices of coronary physiology [index of microcirculatory resistance (IMR) and coronary flow reserve (CFR)] were measured soon after coronary flow restoration by thrombus aspiration and/or balloon predilation.

IMR was measured by using of a conventional pressure wire (Abbott-SJM) soon after coronary flow restoration by thrombus aspiration and/or balloon predilation as previously described using thermodilution technique [7]. IMR values were corrected taking into account coronary wedge pressure measured during stent balloon inflation [11].

Postdilation was left to the operator's discretion. When the operator was satisfied with the procedural result IMR and CFR were measured again and variations of all indices of coronary physiology after stenting ($\Delta IMR = IMR_{pre\text{-}stenting} – IMR_{poststenting}$, $\Delta FFR = FFR_{pre\text{-}stenting} – FFR_{poststenting}$) were determined.

Before completion of the procedure, the pressure wire was withdrawn back close to the guiding catheter to exclude artifact due to pressure drift.

2.5. OCT imaging and segmentation analysis

FD-OCT images were acquired using the FD-OCT Illumiem Optis™ systems with the Dragonfly Duo™ imaging catheters (St. Jude Medical, Westford, MA). Imaging was performed at the same time points chosen for the measurement of IMR using a non-occlusive technique with automated pullback (pullback speed 36 mm/s–75 mm length segment imaged) during a manual intracoronary injection of isoosmolar contrast.

Off-line analysis was carried out using QCU-CMS software (LKEB, Leiden, The Netherlands) by two experienced operators (M.S. and M.A.T) blinded to hemodynamics values.

A common longitudinal region of interest (ROI) was thus identified in both pre- and post-stenting runs. In this report, ROI were the proximal and distal reference segments away from the stented region. (Fig. 1).

Proximal and distal references were defined in the post-stenting runs as the segments not containing major side branches extending for a minimum of 1 mm and a maximum of 5 mm proximally and distally to the edges of the stented segments, respectively.

The pre- and post-stenting runs were, then, exactly matched using anatomical landmarks (i.e., side branches, calcific nodules, etc.) as references for each patient. As confirmation of an accurate matching, references (both proximal and distal) had to be equal in length (same number of frames) in the pre- and post-stenting runs.

After checking and adjusting Z offset, lumen contours were automatically detected with manual correction when necessary. In the post-stenting run, stent struts were first identified then LA, and stent area contours were traced. The analysis was carried out every 1 mm of the whole ROI in both the pre- and post-stenting runs rather than in each cross-section. The global measurements of lumen area were used, rather than lumen area in each cross-section.

2.6. Statistical analysis

Discrete variables are presented as counts and percentages. Continuous variables are presented as mean ± SD or median with interquartile range (IQR) as appropriate after checking for normality distribution using the Shapiro-Wilk test. Correlations were tested using the ρ Spearman coefficient. Normally distributed continuous variables were compared using the *t*-test or t-test for repeated measures, as appropriate, whilst non-normally distributed continuous variables were compared using the Mann-Whitney test or Wilcoxon signed-rank test for repeated measures, as appropriate.

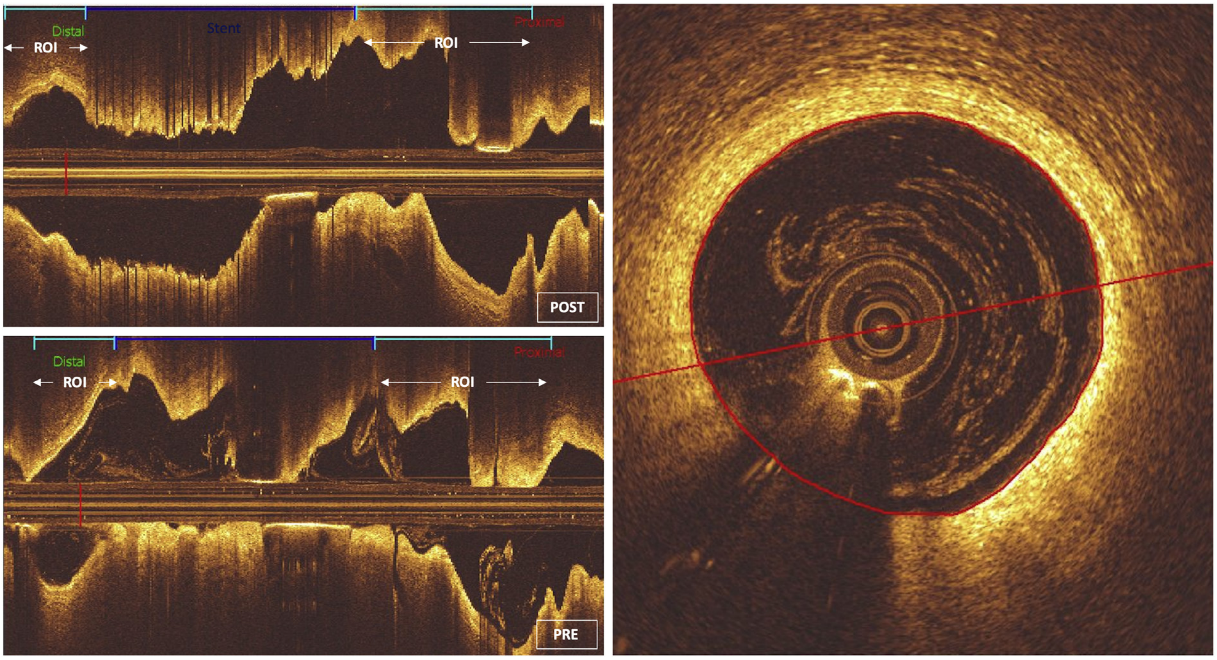

Fig. 1. Method of analysis of optical coherence tomography. Cross-sectional image (right) with longitudinal view of pre- and post-stenting (left) are demonstrated. Red line in the cross section represents lumen area.

Table 1
Baseline clinical characteristics.

Clinical characteristics	Whole cohort (19 patients)
Male gender	16
Age	58 ± 10.7
Hypertension	11
Hypercholesterolemia	7
Diabetes mellitus	1
Active smoker	10
Family history of IHD	7
Previous cardiac history	4
Mean Symptom-onset-to-needle time (min)	220 ± 148.5
<3 h	10
≥3 and <6 h	5
≥6 h	4
Culprit vessel	
LAD	8
LCx	1
RCA	10
TIMI flow at presentation	
0	13
1	4
2	1
3	1
Number of diseased vessels	
1	16
2	3
Thrombus score	
0–1–2	0
3	4
4	12
5	3
SYNTAX score	8 ± 5
Troponin peak (ng/mL)	122.8 ± 81.3
Creatinine (μmol/mL)	72.3 ± 14
GFR	98.4 ± 29.8
Periprocedural medications	
Aspirin	19
Clopidogrel	19
Bivalirudin	19
GPIIbIIIa inhibitors	5
Total adopted	2
Bailout	3

Abbreviations. LAD – left anterior descending artery; LCx – left circumflex artery; RCA – right coronary artery; GFR – glomerular filtration rate.

All statistical analyses were performed using SPSS 22.0 (SPSS, Inc. Chicago, Illinois) and a *p*-value <0.05 was considered statistically significant.

3. Results

3.1. Clinical and procedural characteristics

A total of 19 STEMI patients recruited within the Oxford Acute Myocardial Infarction study and with both presenting and post-stenting FD-OCT and hemodynamic measurements were included in the current analysis. Clinical and procedural characteristics are

Table 2
Procedural characteristics of the study population.

Procedural characteristics	Whole cohort (19 patients)
Thrombus aspiration	17
Pre-dilation	19
Maximum balloon diameter (mm)	2.53 ± 0.2
Pre-stent 2D-QCA	
MLD (mm)	1.37 ± 0.5
MLA (mm)	1.68 ± 1.4
%DS	52.6 ± 11.5
Lesion length (mm)	15.2 ± 6.7
DES	17
Number of stents	
1	18
2	1
Stent length (mm)	25.4 ± 11.5
Stent diameter (mm)	3.4 ± 0.4
Post-dilation	16
Maximum balloon diameter (mm)	3.64 ± 0.4
Final TIMI flow	
2	3
3	16
Incomplete ΣSTR (<70%)	2
MBG	
0–1	3
2	4
3	12

Abbreviations. QCA – quantitative coronary arteriography; DES – drug-eluting stents; ΣSTR – sum of ST-segment resolution; MBG – myocardial blush grade.

Table 3
Pre- and post-procedural blood pressure and index of microcirculatory resistance measurement.

Hemodynamic parameters (mm Hg)		Baseline	Hyperemia
Pre-stenting	Mean arterial pressure	89.9 ± 13.5	81.2 ± 11.6
	Systolic blood pressure	112.6 ± 16.1	104.7 ± 16.3
	Diastolic blood pressure	70.3 ± 11.4	63.4 ± 12.5
Post-stenting	Mean arterial pressure	91.3 ± 17.3	82.6 ± 11.8
	Systolic blood pressure	117.2 ± 20.9	106.5 ± 17.4
	Diastolic blood pressure	71.6 ± 13.1	63.8 ± 12.5
Index of microcirculatory resistance			
Pre-stenting			55.3 ± 38.1
Post-stenting			28.9 ± 17.4
Coronary flow reserve			
Pre-stenting			1.1 ± 0.23
Post-stenting			1.3 ± 0.49

summarized in Tables 1 and 2. 84.2% of enrolled patients were men with a mean age of (58 ± 10.7 years). Majority of the patients had been treated within 6 h of symptom onset (78.9%) with a mean symptom-onset-to-needle time of 2.5 h (IQR 3.3 h). Roughly two-thirds (57.8%) had hypertension, and nearly one-third had a history of hyperlipidemia (36.8%) with only a small proportion of patients had an established diagnosis of diabetes mellitus (5.2%). Of the selected cohort, only a few patients (15.7%) were observed to have a very large angiographic thrombotic burden (thrombus score 5). Thrombus aspiration (89.4%), second-generation drug-eluting stents (89%) and post-dilation (84.2%) were used in the vast majority of cases. The occurrence of MBG < 2 and or incomplete ST-segment recovery (ΣSTR) was detected in 10.6% of these patients.

Out of 19 pre- and post-stenting OCT runs, the distal segment was not appropriate for analysis in 2 cases, and three runs had unsuitable distal segments.

3.2. Hemodynamic parameters

The baseline mean SBP was (112.6 mm Hg ± 16.1) and (117.2 mm Hg ± 20.9), pre- and post-stenting, respectively. The baseline mean MAP (89.9 mm Hg ± 13.5) and (91.3 mm Hg ± 17.3), pre- and post-stenting, respectively.

We have also evaluated the pre- and post-PCI changes in the intracoronary pressure [i.e., mean distal pressure (Pd)]. The mean Pd was (71.9 mm Hg ± 17.9) and (87 mm Hg ± 19.7), pre- and post-stenting, respectively. Complete parameters of coronary physiology before and after stenting, including SBP, SBP, and MAP at both baseline and after hyperemia induction as well as IMR and CFR data are summarized in Table 3.

3.3. FD-OCT derived parameters

We explored the changes in dimensions of the proximal and distal reference segments before and after stenting. Pre-and post-stenting FD-OCT-derived lumen parameters of the proximal and distal references as well as of the stented segments are summarized in Table 4.

In the proximal segments, pre-stenting mean average LA was larger compared to post-stenting mean average LA (8.46 ± 2.91 mm^2 vs. 7.8 ± 2.79 mm^2; $p = 0.032$). On the other hand, these differences were not observed in the distal segment (5.46 ± 2.48 mm^2 vs. 5.78 ± 2.49 mm^2; $p = 0.193$) for the Pre-and post-stenting segment, respectively.

3.4. Relationship between the hemodynamic parameters and FD-OCT derived measures

The range of the observed SBP differences (between pre- and post-PCI) went from −25 to +23 mm Hg. Similar differences were observed in the MAP, with the range of the observed MAP differences (between pre- and post-PCI) going from −32 to +15 mm Hg. There were poor correlations between these changes in the pre- and post-stenting hemodynamic parameters (i.e., SBP, DBP, and MAP) and the mean average LA and mean minimal LA as well as with the mean average LD and mean minimal LD (Table 5). The relationship between delta blood pressure and delta OCT parameters are demonstrated in Fig. 2–4. The significant variability in the blood pressure values (pre- and post-stenting) resulted only in minimal changes in the FD-OCT derived lumen measurements. The relationship and correlations between the change in pre- and post-stenting hemodynamic parameters and FD-OCT derived parameters are summarized in Table 5.

4. Discussion

The main findings of our report are summarized as follows: [1] baseline measurements of coronary arterial lumen size at reference sites

Table 4
Pre- and post-procedural optical coherence tomography characteristics.

Pre-stenting		Post-stenting		p-Value
Reference segments (proximal plus distal)				
Average LA (mm^2)	7.12 ± 2.5	Average LA (mm^2)	6.8 ± 2.3	0.20
Minimal LA (mm^2)	3.86 ± 1.9	Minimal LA (mm^2)	3.91 ± 1.8	0.82
Average LD (mm^2)	2.92 ± 0.5	Average LD (mm^2)	2.86 ± 0.5	0.26
Minimal LD (mm^2)	2.75 ± 0.6	Minimal LD (mm^2)	2.61 ± 0.4	0.19
Proximal references				
Average LA (mm^2)	8.46 ± 2.9	Average LA (mm^2)	7.8 ± 2.7	0.03
Minimal LA (mm^2)	6.06 ± 2.2	Minimal LA (mm^2)	5.8 ± 2.4	0.23
Average LD (mm^2)	3.22 ± 0.5	Average LD (mm^2)	3.09 ± 0.5	0.04
Minimal LD (mm^2)	2.98 ± 0.5	Minimal LD (mm^2)	2.83 ± 0.5	0.03
Distal references				
Average LA (mm^2)	5.46 ± 2.4	Average LA (mm^2)	5.78 ± 2.4	0.19
Minimal LA (mm^2)	3.33 ± 1.6	Minimal LA (mm^2)	3.55 ± 1.9	0.59
Average LD (mm^2)	2.54 ± 0.6	Average LD (mm^2)	2.62 ± 0.5	0.20
Minimal LD (mm^2)	2.41 ± 0.7	Minimal LD (mm^2)	2.37 ± 0.5	0.70
Stented segments				
Average stent area (mm^2)				9.62 ± 2.5
Minimal stent area (mm^2)				7.89 ± 2.5
Average stent diameter (mm^2)				3.46 ± 0.4
Minimal stent diameter (mm^2)				3.13 ± 0.5

Abbreviations. LA — lumen area; LD — lumen diameter.

Table 5
The correlation between the blood pressure changes and the changes in the optical coherence tomography lumen measurements.

Hemodynamic parameters (mm Hg)				Delta SBP = 4.5 ± 12.4	Delta DBP = 1.2 ± 10.2	Delta MAP = 1.3 ± 10.5
FD-OCT measurements (mm^2)	Total Reference segments *(Proximal + Distal)*	Δ Minimal LA	0.04 ± 0.8	*R* = 0.14, *P* = 0.54	R = 0.43, P = 0.06	*R* = 0.31, *P* = 0.18
		Δ Average LA	−0.31 ± 1.0	*R* = 0.17, *P* = 0.48	*R* = 0.24, *P* = 0.31	*R* = 0.22, *P* = 0.34
		Δ Minimal LD	−0.13 ± 0.4	*R* = 0.15, *P* = 0.53	*R* = 0.25, *P* = 0.28	*R* = 0.32, P = 0.18
		Δ Average LD	−0.05 ± 0.2	*R* = 0.19, *P* = 0.42	*R* = 0.28, *P* = 0.23	*R* = 0.26, P = 0.28
	Proximal references	Δ Minimal LA	−0.25 ± 0.8	*R* = 0.02, *P* = 0.92	R = -0.05, *P* = 0.83	R = 0, *P* = 1.00
		Δ Average LA	−0.66 ± 1.1	R = -0.06, *P* = 0.82	*R* = 0.15, *P* = 0.55	*R* = 0.07, *P* = 0.76
		Δ Minimal LD	−0.14 ± 0.2	R = -0.01, *P* = 0.99	*R* = 0.11, *P* = 0.66	*R* = 0.10, *P* = 0.70
		Δ Average LD	−0.13 ± 0.2	R = -0.05, *P* = 0.84	R = 0.17, *P* = 0.49	R = 0.14, *P* = 0.58
	Distal references	Δ Minimal LA	0.22 ± 1.6	R = 0, P = 1.00	*R* = 0.12, *P* = 0.65	R = -0.01, *P* = 0.96
		Δ Average LA	0.31 ± 0.9	R = 0.07, P = 0.76	R = -0.10, P = 0.70	R = -0.19, P = 0.48
		Δ Minimal LD	−0.04 ± 0.4	R = 0.10, P = 0.70	R = -0.11, *P* = 0.68	R = -0.08, *P* = 0.74
		Δ Average LD	0.07 ± 0.2	R = 0.14, P = 0.58	R = -0.14, *P* = 0.59	R = -0.24, *P* = 0.36

Abbreviations. R – Pearson's correlation coefficient; FD-OCT – Fourier domain optical coherence tomography; SBP – systolic blood pressure; DBP – diastolic blood pressure; MAP – mean arterial blood pressure; LA – lumen area; LD – lumen diameter; Δ represents the difference at the end of the coronary intervention (post-stenting) and just before the coronary intervention (pre-stenting).

with FD-OCT are different from post-interventional treatment measurements; [2] coronary arterial lumen measurements changes (from pre- to post-PCI) were minimal irrespective of the degree of the blood pressure changes pre- and post-intervention; [3] no correlation was observed between hemodynamic parameters and FD-OCT derived measures.

It is clinical apparent that STEMI patients do have different blood pressure levels before and after reperfusion and intravascular imaging

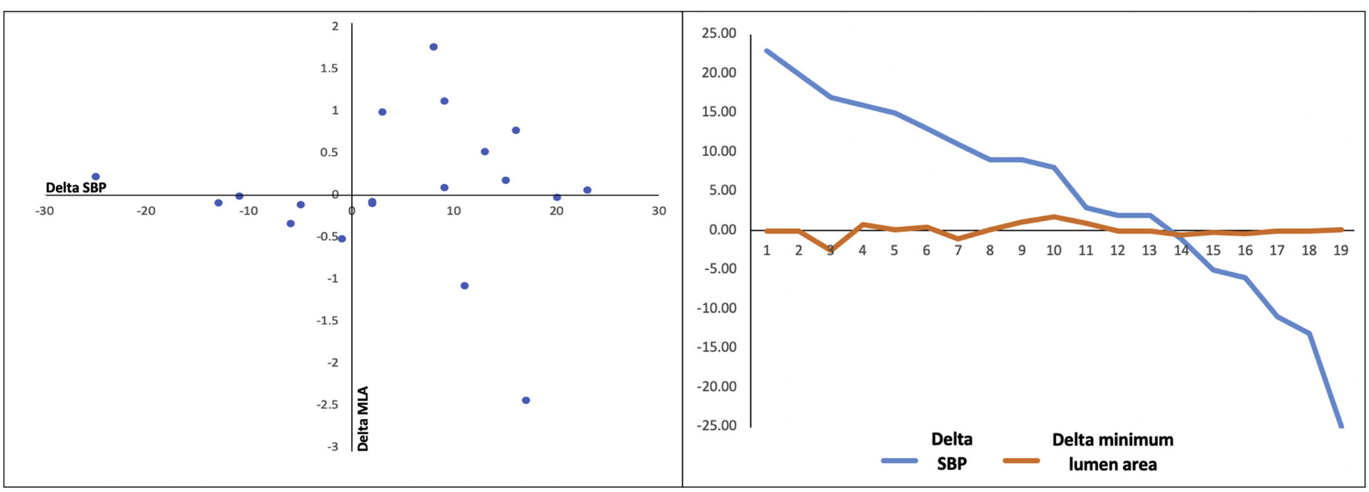

Fig. 2. Relationship between the pre- and post-stenting systolic blood pressure and the minimum lumen area – (left) scatter plot; (right) line graph where the x-axis represents individual patients.

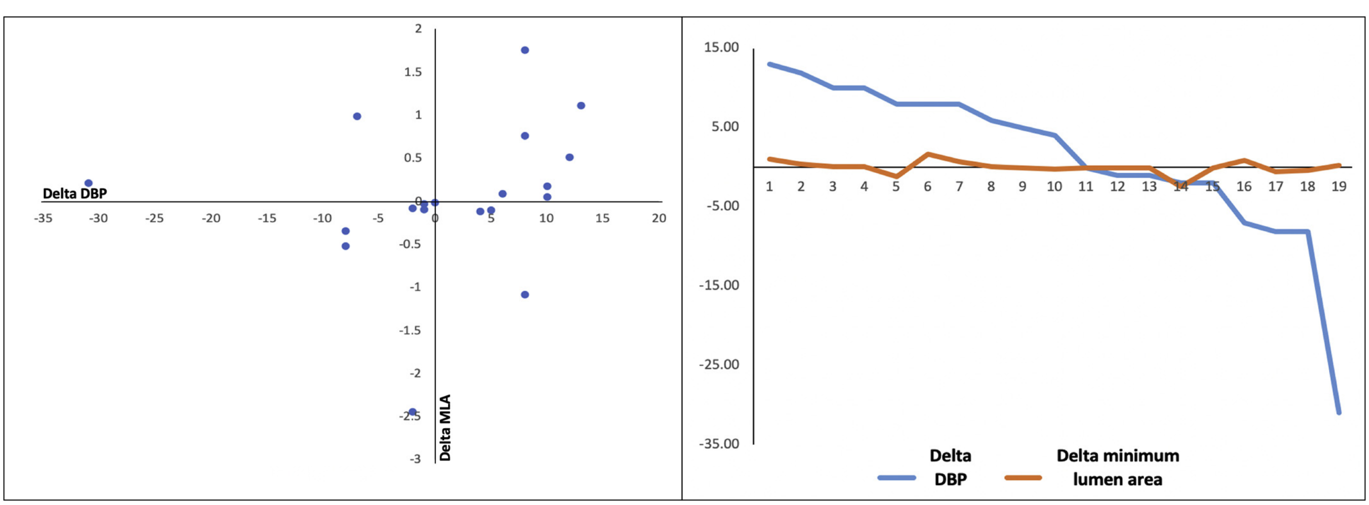

Fig. 3. Relationship between the pre- and post-stenting diastolic blood pressure and the minimum lumen area – (left) scatter plot; (right) line graph where the x-axis represents individual patients.

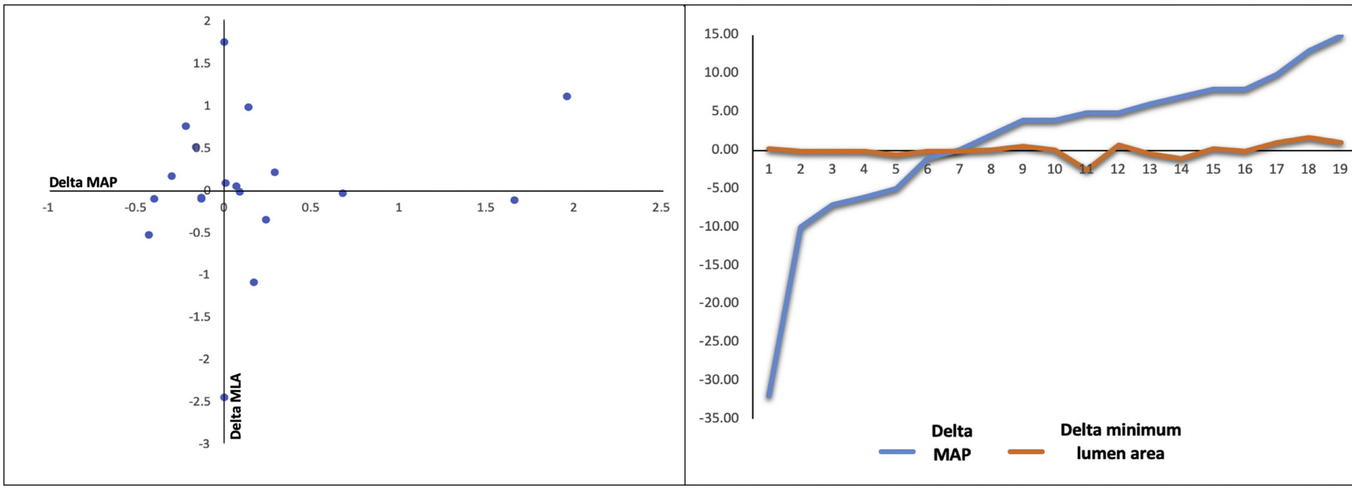

Fig. 4. Relationship between the pre- and post-stenting mean arterial pressure and the minimum lumen area – (left) scatter plot; (right) line graph where the x-axis represents individual patients.

is typically suggested to investigate the culprit lesion and to inform stent selection [12]. The latter is achieved by measuring the reference segments in terms of lumen-to-lumen or EEM-to-EEM dimensions depending on operator preferences. The impact of blood pressure variability on those dimensions remains uncertain.

As of yet, there has not been publication exploring the impact of those hemodynamic changes on OCT measurements. Moreover, only a few publications have examined the changes of lumen dimensions of the infarct-related artery before and after the intervention with conflicting results [13,14].

Using FD-OCT measurements, Kurokawa et al. [15] found that the average LD and LA of the distal reference site were significantly increased after PCI with stent implantation. By contrast, these indices at the proximal reference site were significantly decreased.

In our study, the baseline measurements of coronary arterial lumen size at reference sites with FD-OCT are different from post-interventional treatment measurements; however, these changes in the luminal measurements (from pre- to post-PCI) were negligible with no correlation to the degree of the blood pressure changes pre- and post-intervention.

One phenomenon that could explain our findings is "coronary autoregulation" where coronary blood flow remains relatively constant over a wide range of perfusion pressures [16]. This tight control of the blood flow is characterized by adjustments in vascular resistance mainly due to autoregulation in the coronary circulation that results from the concerted interaction of several different mediators or mechanisms [17–20].

Both metabolic and myogenic theories have been proposed to explain the autoregulation of coronary flow. Based on the metabolic theory, a decrease in coronary artery pressure reduces flow, which results in coronary vasodilation by decreasing myocardial substrate availability or increasing production of metabolites [16–18]. While according to the myogenic theory, an intrinsic mechanism in vascular smooth muscle regulates resistance in response to changes in transmural pressure thus can change coronary vessel diameter in response to pressure. Hence, a decrease in coronary artery pressure results in coronary vasodilation independent of changes in blood flow [19,21,22] [19–21].

Nevertheless, these firm coronary autoregulation mechanisms prevail in the microvasculature and the smaller arterioles rather than the epicardial coronary vessels that were studied in our report, making it less likely to solely explain our findings.

The index of microcirculatory resistance (IMR) was proposed and validated for assessing the status of microcirculation [23]. In order to account for any microcirculatory changes that can affect the coronary

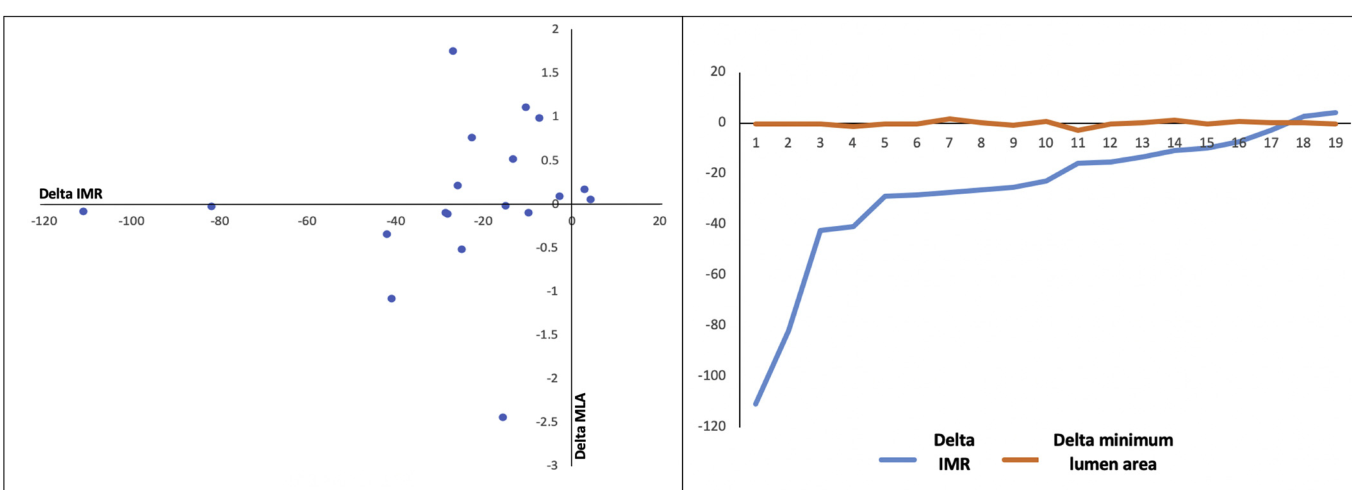

Fig. 5. Relationship between the pre- and post-stenting the index of microcirculatory resistance and the minimum lumen area – (left) scatter plot; (right) line graph where the x-axis represents individual patients. Abbreviation. ROI – region of interest; MLA – minimum lumen area; SBP – systolic blood pressure; DBP – diastolic blood pressure; MAP – mean arterial blood pressure; IMR – index of microcirculatory resistance.

lumen measurements we observed, we used IMR to assess the pre- and post-procedural microvascular impairment. We found no significant correlations between the IMR pre- and post-stenting and the FD-OCT derived minimum LA ($R = 0.404$, $p = 0.087$) (Fig. 5). Similar results were noted when investigating the associations of minimum LA with CFR ($R = 0.061$, $p = 0.803$).

Additionally, we have examined the pre- and post-PCI changes as well in the intracoronary pressure in relation to FD-OCT derived lumen measurement. Similar to systemic blood pressure, there was no relation between intracoronary pressure [i.e., mean distal pressure (Pd)] variability and lumen measurements (correlation with minimum LA: $R = 0.431$, $p = 0.065$; Supplemental Fig. 1).

It should be noted that the FD-OCT was performed in our study immediately after stenting thus these results might have changed if these measurements were performed at a later stage once the adrenergic "storm" and the thrombotic burden resolved. Sahin et al. [13] showed that reference vessel diameter (RVD) was higher during follow-up coronary angiography a few days after STEMI in patients who underwent PPCI with simple balloon dilatation and/or thrombus aspiration. On the other hand, Cristea et al. [14] evaluated 2974 patients with STEMI and reported a very small difference in RVD of the infarct-related arteries using quantitative coronary angiography at baseline or post-PCI. Very similar to our results, RVD increased to a small degree from baseline to post-PCI (absolute change median 0.06 mm) and returned to baseline values by the follow-up angiogram (at a mean time of 13 months).

4.1. Clinical implications

FD-OCT is known to provide accurate measurements of coronary lumen size with excellent reproducibility [24]. Based on our results, these measurements seem to be reliable despite the extreme hemodynamic changes that might occur in patients undergoing coronary intervention after an acute STEMI. This would give the PCI operator higher confidence to integrate the FD-OCT data into decision-making processes.

4.2. Limitations

We acknowledge that the sample size is small, however, this should not impact on our final conclusions since there was no heterogeneity in the observed changes in luminal dimensions; on the other hand, only 2 values of the blood pressure were recorded, pre- and post-PCI; continuous measurement of the BP at both phases and evaluation of its variability may offer different insights. Additionally; the range of change in blood pressure observed was rather relatively small.

5. Conclusion

In PPCI, despite blood pressure variability, the difference in lumen cross-sectional area, between pre- and post-coronary artery stenting was minimal. This study supports the use of FD-OCT lumen areas to reliably and accurately inform clinical decisions during PPCI.

Supplementary data to this article can be found online at https://doi.org/10.1016/j.carrev.2019.05.027.

References

[1] Bezerra HG, Costa MA, Guagliumi G, Rollins AM, Simon DI. Intracoronary optical coherence tomography: a comprehensive review clinical and research applications. JACC Cardiovasc Interv 2009;2(11):1035–46.

[2] Prati F, Regar E, Mintz GS, Arbustini E, Di Mario C, Jang IK, et al. Expert review document on methodology, terminology, and clinical applications of optical coherence tomography: physical principles, methodology of image acquisition, and clinical application for assessment of coronary arteries and atherosclerosis. Eur Heart J 2010;31(4):401–15.

[3] van der Sijde JN, Karanasos A, van Ditzhuijzen NS, Okamura T, van Geuns RJ, Valgimigli M, et al. Safety of optical coherence tomography in daily practice: a comparison with intravascular ultrasound. Eur Heart J Cardiovasc Imaging 2017;18(4):467–74.

[4] Prati F, Cera M, Ramazzotti V, Imola F, Giudice R, Giudice M, et al. From bench to bedside: a novel technique of acquiring OCT images. Circulation journal: official journal of the Japanese Circulation Society 2008;72(5):839–43.

[5] Karanasos A, Ligthart J, Witberg K, van Soest G, Bruining N, Regar E. Optical coherence tomography: potential clinical applications. Current Cardiovascular Imaging Reports 2012;5(4):206–20.

[6] Tearney GJ, Regar E, Akasaka T, Adriaenssens T, Barlis P, Bezerra HG, et al. Consensus standards for acquisition, measurement, and reporting of intravascular optical coherence tomography studies: a report from the International Working Group for Intravascular Optical Coherence Tomography Standardization and Validation. J Am Coll Cardiol 2012;59(12):1058–72.

[7] De Maria GL, Cuculi F, Patel N, Dawkins S, Fahrni G, Kassimis G, et al. How does coronary stent implantation impact on the status of the microcirculation during primary percutaneous coronary intervention in patients with ST-elevation myocardial infarction? Eur Heart J 2015;36(45):3165–77.

[8] Sianos G, Papafaklis MI, Serruys PW. Angiographic thrombus burden classification in patients with ST-segment elevation myocardial infarction treated with percutaneous coronary intervention. J Invasive Cardiol 2010;22(10):6b–14b Suppl B.

[9] Napodano M, Ramondo A, Tarantini G, Peluso D, Compagno S, Fraccaro C, et al. Predictors and time-related impact of distal embolization during primary angioplasty. Eur Heart J 2009;30(3):305–13.

[10] Sorajja P, Gersh BJ, Costantini C, McLaughlin MG, Zimetbaum P, Cox DA, et al. Combined prognostic utility of ST-segment recovery and myocardial blush after primary percutaneous coronary intervention in acute myocardial infarction. Eur Heart J 2005;26(7):667–74.

[11] Layland J, MacIsaac AI, Burns AT, Somaratne JB, Leitl G, Whitbourn RJ, et al. When collateral supply is accounted for epicardial stenosis does not increase microvascular resistance. Circ Cardiovasc Interv 2012;5(1):97–102.

[12] Neumann F-J, Sousa-Uva M, Ahlsson A, Alfonso F, Banning AP, Benedetto U, et al. 2018 ESC/EACTS Guidelines on myocardial revascularization. European heart journal. 2019;40(2):87–165.

[13] Sahin M, Demir S, Kocabay G, Bulut M, Alici G, Ozkan B, et al. Coronary vessel diameters during and after primary percutaneous coronary artery intervention. Herz 2014;39(4):515–21.

[14] Cristea E, Stone GW, Mehran R, Kirtane AJ, Brener SJ. Changes in reference vessel diameter in ST-segment elevation myocardial infarction after primary percutaneous coronary intervention: implications for appropriate stent sizing. Am Heart J 2011;162(1):173–7.

[15] Kurokawa M, Uemura S, Watanabe M, Dote Y, Sugawara Y, Goryo Y, et al. Changes in the reference lumen size of target lesions before and after coronary stent implantation: evaluation with frequency domain optical coherence tomography. International journal of cardiology Heart & vasculature 2015;8:122–7.

[16] van de Hoef TP, Nolte F, Rolandi MC, Piek JJ, van den Wijngaard JPHM, Spaan JAE, et al. Coronary pressure-flow relations as basis for the understanding of coronary physiology. J Mol Cell Cardiol 2012;52(4):786–93.

[17] Dole WP. Autoregulation of the coronary circulation. Prog Cardiovasc Dis 1987;29(4):293–323.

[18] Kuo L, Chilian WM, Davis MJ. Interaction of pressure- and flow-induced responses in porcine coronary resistance vessels. Am J Physiol 1991;261(6 Pt 2):H1706–15.

[19] Kuo L, Chilian WM, Davis MJ. Coronary arteriolar myogenic response is independent of endothelium. Circ Res 1990;66(3):860–6.

[20] Kanatsuka H, Lamping KG, Eastham CL, Marcus ML. Heterogeneous changes in epimyocardial microvascular size during graded coronary stenosis. Evidence of the microvascular site for autoregulation. Circ Res 1990;66(2):389–96.

[21] Rajagopalan S, Dube S, Canty Jr JM. Regulation of coronary diameter by myogenic mechanisms in arterial microvessels greater than 100 microns in diameter. Am J Physiol 1995;268(2 Pt 2):H788–93.

[22] Miller Jr FJ, Dellsperger KC, Gutterman DD. Myogenic constriction of human coronary arterioles. Am J Physiol 1997;273(1):H257–64 Pt 2.

[23] Fearon WF, Balsam LB, Farouque HM, Caffarelli AD, Robbins RC, Fitzgerald PJ, et al. Novel index for invasively assessing the coronary microcirculation. Circulation 2003;107(25):3129–32.

[24] Kubo T, Akasaka T, Shite J, Suzuki T, Uemura S, Yu B, et al. OCT compared with IVUS in a coronary lesion assessment. the OPUS-CLASS study JACC Cardiovascular imaging 2013;6(10):1095–104.